Dyes and Pigments 98 (2013) 11–16

Contents lists available at SciVerse ScienceDirect

Dyes and Pigments

journal homepage: www.elsevier.com/locate/dyepig

A new isoindigo-based molecule with ideal energy levels for solution-processable organic solar cells

Ting Wang [a], Yanhua Chen [a,b], Xichang Bao [a], Zhengkun Du [a], Jing Guo [a], Ning Wang [a], Mingliang Sun [b,*], Renqiang Yang [a,*]

[a] Qingdao Institute of Bioenergy and Bioprocess Technology, Chinese Academy of Sciences, Qingdao 266101, China
[b] Institute of Material Science and Engineering, Ocean University of China, Qingdao 266100, China

ARTICLE INFO

Article history:
Received 17 December 2012
Received in revised form
31 January 2013
Accepted 1 February 2013
Available online 21 February 2013

Keywords:
Isoindigo
Thieno[3,2-*b*]thiophene
Organic photovoltaic effect
Low bandgap
Small molecule
Energy level

ABSTRACT

A new easily-accessible solution-processed oligomer, with an isoindigo group as an electron acceptor and a thieno[3,2-*b*]thiophene flanked by thiophenes as electron donors, has been synthesized by a Stille coupling reaction. Through introducing the extended π-conjugated groups into isoindigo, the electro-optical properties of the material can be fine-tuned. The isoindigo oligomer has a broad absorption in the region from 300 to 800 nm with a narrow bandgap (1.54 eV), which is believed to be an ideal bandgap as donor materials. The oligomer possesses low HOMO energy level (−5.39 eV). The potential of optical and electronic properties encouraged us to explore the photovoltaic performance using the oligomer as the donor material in bulk heterojunction organic solar cell along with 6,6-phenyl-C61-butyric acid methyl ester as the acceptor. The solar cell based on the oligomer with an inverted device configuration provided a power conversion efficiency of 1.41% under the AM 1.5G illumination with an intensity of 100 mW cm^{-2} from a solar simulator.

1. Introduction

In the past decade organic photovoltaics (OPVs) have achieved remarkable progress due to unique advantages such as low cost, light weight and applications in flexible large-area devices [1–4]. At present intensive efforts have been dedicated to improving the power conversion efficiencies (PCEs) of polymer bulk heterojunction (BHJ) architectures, and their PCEs have gradually exceeded 7% [5–8]. Despite these advancements, the efficiency of a polymer-fullerene solar cell device is limited by factors such as complex synthesis and unknown long-term stability [9], so there remains a significant challenge for OPVs toward commercialization. An emerging alternative to polymer BHJ solar cells involves the use of solution-processed small molecule BHJ which combine the advantages of well-defined chemical structure, reproducible synthesis, high purification, and more straightforward analysis of structure property relationships [10–12]. A combination of structural design, morphology control, and device engineering has led to PCEs reaching the 6–7% for soluble small molecule solar cells [13,14].

The PCEs of the OPVs are proportional to open circuit voltage (V_{OC}), short circuit current density (J_{SC}), and fill factor (*FF*). The three parameters interplay each other, for example, V_{OC} is mainly related to the energy level difference between the LUMO of the acceptor and the HOMO of the donor [15]. However, sometimes, a lower HOMO level of the donor would lead to an increased bandgap and less efficient light absorption. High V_{OC} and high J_{SC} are difficult to obtain concurrently [16]. In order to achieve higher PCEs, a delicate balance between the bandgap and energy level is needed via judicious control over the physical properties of a donor [17]. 6,6-phenyl-C61-butyric acid methyl ester (PCBM) has a LUMO energy level of −4.2 eV. It is estimated that a minimum LUMO energy difference of 0.3 eV between the donor and the acceptor is required to facilitate exciton splitting and charge dissociation [18]. Accordingly, it is believed that the ideal lowest possible LUMO level of the donor would be near −3.9 eV [19]. Furthermore, low bandgap materials can absorb more light, increasing the J_{SC}. However, lowering the bandgap requires an increase of the HOMO which would reduce V_{OC} normally. Thus an optimal bandgap of 1.5 eV is proposed to be a compromise between the two competing factors. Consequently, the HOMO of the "ideal" donor would be around −5.4 eV [3,19] (Fig. 1). Following the basic requirements and scientific issues in the molecular design mentioned above, it is important to synthesize materials with an ideal bandgap and energy level for further increasing photovoltaic performance.

Isoindigo (ID) which has been used in the dye industry for a long time [20] has some advantages similar to diketopyrrolopyrroles

* Corresponding authors.
E-mail addresses: mlsun@ouc.edu.cn (M. Sun), yangrq@qibebt.ac.cn (R. Yang).

0143-7208/$ – see front matter © 2013 Elsevier Ltd. All rights reserved.
http://dx.doi.org/10.1016/j.dyepig.2013.02.003

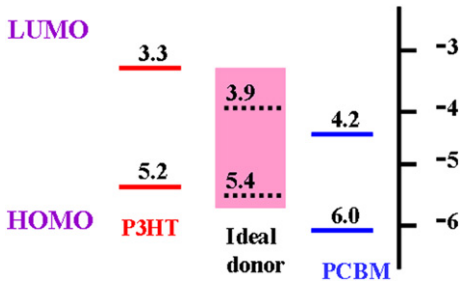

Fig. 1. Electronic energy levels of P3HT, ideal donor and PCBM.

(DPP) [21–24], such as strong electron-withdrawing ability (derived from its two lactam rings), low HOMO levels, relatively small bandgaps and planar architectures. Meanwhile, compared to DPP, isoindigo can be obtained easily from various natural sources, and also has much better solubility than DPP. It seems that isoindigo is suitable for OPVs, yet the application of isoindigo in organic solar cells was first introduced in 2011 [25], with state-of-the-art isoindigo-based BHJ solar cells reaching a PCE of 6.3% [26]. This result shows particular potential of isoindigo as an electron-deficient unit toward high efficient OPVs. Until now most of the research about isoindigo has focused on polymer solar cells, while there are few reports on isoindigo-based small molecules except for one example reported by Reynolds et al. recently [27]. However, the optical bandgap of isoindigo-based materials is too large and the HOMO level is not low enough to afford a high V_{OC}, so it will make sense to fine-tune the optical and electronic properties of isoindigo derivatives through molecular design.

In this work we focus on the design and synthesis of a new isoindigo-based molecule with ideal optical and electrical properties in order to significantly increase the photovoltaic performance of the material. The incorporation of fused thiophenes and other aromatic structures into conjugated architectures would increase planarity and rigidity which will lead to a lower optical bandgap [28–30]. The rigid and coplanar thieno[3,2-*b*]thiophene (TT) consists two fused thiophenes and the material based on a TT unit shows high hole mobility and good light absorption because of closely π stacking in the solid state [31–33]. On the basis of the above consideration, in this contribution, TT unit was incorporated with isoindigo to achieve a new easily-accessible and fully solution-processed small molecule donor IDTTT (see Scheme 1 for its molecular structure). The conjugated component, TT unit, will increase the conjugation length of the donor, thus make the new molecule close to an ideal model. 2-ethylhexyl was selected as a substitute to improve the solubility. As we know, inverted solar cells have some advantages superior to regular device structure, such as interface stability, a stable metal electrode, design flexibility for tandem or stacked cells [34–36]. Therefore, we will explore the inverted solar cells using the new molecule IDTTT and PCBM blending as the active layer. This is the first example for isoindigo-based materials applied in inverted structure.

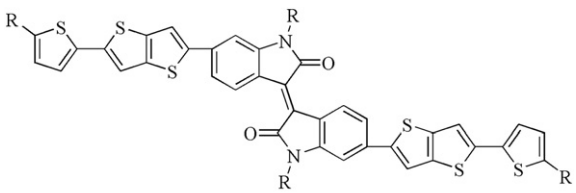

Scheme 1. Chemical structure of isoindigo-based molecule IDTTT.

2. Experimental

2.1. Materials and characterization methods

All reagents and starting materials were purchased from J&K, Alfa Aesar and used without further purification, unless otherwise noted. Solvents were distilled before use. Thieno[3,2-*b*]thiophene (**1**) [37], (E)-6,6′-dibromoisoindigo (**4**) [38] and 2-trimethylstannane-5-(2-ethylhexyl)thiophene (**8**) [39] were prepared according to the literature methods. ^{1}H NMR and ^{13}C NMR spectra were recorded on Bruker DRX-600 (600 MHz) spectrometer. FT-IR spectra were taken on a Nicolet 6700 spectrophotometer by using KBr pellets. High resolution mass spectra were recorded under APCI mode on a Bruker Maxis UHR TOF spectrometer. UV–vis spectra were measured on a Varian Cary 50 UV/vis spectrometer. Surface roughness and morphology of thin films were characterized by atomic force microscopy (AFM) on an Agilent 5400. Cyclic voltametry (CV) was performed by a CHI 660D System with a three-electrode cell in a solution of 0.10 M tetrabutylammonium hexafluorophosphate ($TBAPF_6$) in dichloromethane (DCM) solution at a scan rate of 100 mV/s. The film thickness was measured by a Veeco Dektak 150 surface profiler. The current density–voltage (*J–V*) characteristics were recorded with a Keithley 2420 source measurement unit under simulated 100 mW/cm^2 (AM 1.5G) irradiation from a Newport solar simulator.

2.2. Device fabrication and characterization

The inverted photovoltaic devices were prepared and characterized. All cells were fabricated on ITO-coated glass substrates with a nominal sheet resistance of 15 Ω/sq. The substrates were cleaned in an ultrasonic bath with detergent, ultra-pure water, acetone, and isopropyl alcohol for 20 min, respectively, and dried in a laboratory oven at 80 °C for one night. The ZnO solution was prepared using zinc acetate and the equally molar monoethanolamine dissolved in 2-methoxyethanol, and then the mixture was stirred vigorously at 60 °C to yield a homogeneous transparent solution. The ITO surfaces were coated by the above ZnO solutions with spin speeds at 2000 rmp for 40 s, and then, baked in an oven at 100 °C for 16 h. A blend solution of IDTTT and 6,6-phenyl-C61-butyric acid methyl ester (PCBM) (American Dye Sources Inc.) with different weight ratios (at a total solids concentration of 20 mg/mL) were prepared in deoxygenated anhydrous chlorobenzene (Sigma–Aldrich) and stirred in a nitrogen filled glove box for 4 h, and then spin-coated on ZnO-coated ITO substrate to form the active layer (~90 nm) in glove box. Subsequently, MoO_3 (3 nm) and Ag (80 nm) were thermal evaporated followed by post-annealing at 120 °C for 10 min. The cathode area defines active area of the devices, which is 0.1 cm^2.

2.3. Synthesis of isoindigo-based oligomer IDTTT

2.3.1. Synthesis of triisopropyl(thieno[3,2-b]thien-2-yl)silane (**2**)

In a dry flask *n*-butyllithium (2.4 M in *n*-hexane, 1.25 mL, 3.0 mmol) was added dropwise to a solution of the thieno[3,2-*b*]thiophene (**1**, 420 mg, 3.0 mmol) in tetrahydrofuran (THF, 20 mL) at 0 °C under nitrogen atmosphere (Scheme 2). After 1 h of stirring at this temperature, neat triisopropyl chlorosilane (0.74 mL, 3.45 mmol) was added dropwise. The solution was stirred for another 3 h and allowed to warm to room temperature, followed by dilution with hexane and washing with water and brine. The organic layer was collected and dried over anhydrous Na_2SO_4. After the solvent was removed in vacuo, the residue was purified by column chromatography on silica gel, eluting with hexane to yield silyl compound **2** (774 mg, 87%) as a white solid. ^{1}H NMR (600 MHz,

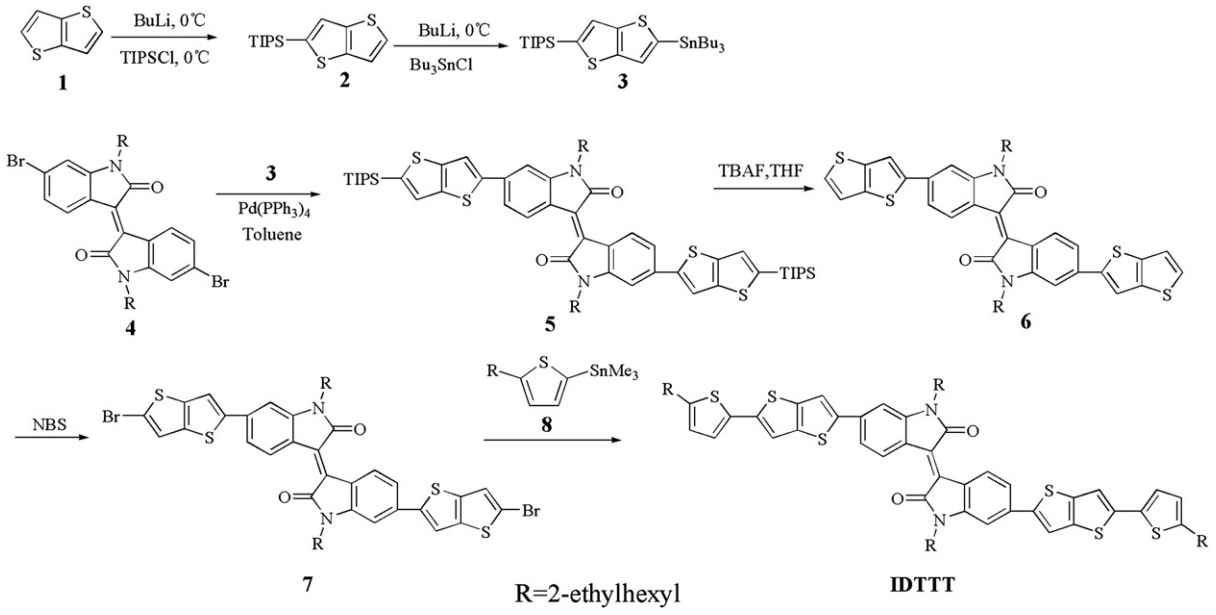

Scheme 2. Synthetic routes for the oligomer IDTTT.

$CDCl_3$) δ 7.39 (d, $J = 5.4$ Hz, 1H), 7.37 (s, 1H), 7.25 (d, $J = 5.4$ Hz, 1H), 1.37 (m, 3H), 1.13 (d, $J = 7.8$ Hz, 18H); ^{13}C NMR (150 MHz, $CDCl_3$) δ 144.6, 141.2, 138.0, 127.9, 126.9, 119.1, 18.6, 11.8.

*2.3.2. Synthesis of triisopropyl(5-(tributylstannyl)thieno[3,2-b] thiophen-2-yl)silane (**3**)*

In a dry flask, *n*-butyllithium (2.4 M in *n*-hexane, 2.5 mL, 6.0 mmol) was added dropwise to a solution of compound **2** (1.78 g, 6 mmol) in 60 mL THF at 0 °C under N_2 atmosphere. After 1 h of stirring at this temperature, neat tributylstannyl chloride (1.6 mL, 6.0 mmol) was added dropwise. The solution was stirred for another 12 h and allowed to warm to room temperature, followed by dilution with hexane and washing with brine. The organic layer was collected and dried over anhydrous Na_2SO_4. The crude stannyl product **3** was obtained after removing the solvent in vacuo and used directly in the next step without further purification.

*2.3.3. Synthesis of N,N′-bis-(2-ethylhexyl)-3,3′-(5-(triisopropylsilyl) thieno[3,2-b]-thiophen-2-yl)isoindigo (**5**)*

To a solution of compound **3** (4.08 g, 6.97 mmol) and **4** (2.03 g, 3.15 mmol) in anhydrous tetrahydrofuran (THF, 50 mL) bubbled with nitrogen, $Pd(PPh_3)_4$ (30 mg, 0.026 mmol) was added in one portion. The mixture was stirred overnight at 110 °C under nitrogen. Then the mixture was cooled to room temperature and the solution was concentrated to dryness. The crude product was purified by chromatography on silica gel to afford the desired purple product **5** (2.56 g, 75.7%). ^{1}H NMR (600 MHz, $CDCl_3$) δ 9.16 (d, $J = 8.4$ Hz, 2H), 7.58 (s, 2H), 7.38 (s, 2H), 7.32 (d, $J = 8.4$ Hz, 2H), 6.98 (s, 2H), 3.71 (m, 4H), 1.88 (m, 2H), 1.37 (m, 6H), 1.17 (d, $J = 7.2$ Hz, 36H), 1.42–0.82 (m, 28H); ^{13}C NMR (150 MHz, $CDCl_3$) δ 168.6, 146.5, 145.8, 145.4, 141.0, 139.4, 138.5, 131.9, 130.2, 127.1, 121.3, 119.2, 116.2, 104.9, 44.0, 38.0, 31.0, 28.9, 24.4, 23.1, 18.6, 14.1, 11.8, 10.8; IR (KBr, cm^{-1}): 1695 (C=O), 1610 (C=C); APCI-MS $[M + H]^+$ calculated for $C_{62}H_{87}N_2O_2S_4Si_2^+$ *m/z*: 1075.5183, found: 1075.5189.

*2.3.4. Synthesis of N,N′-bis-(2-ethylhexyl)-3,3′-(thieno[3,2-b] thiophen-2-yl)isoindigo (**6**)*

Tetrabutylammonium fluoride trihydrate (4.93 g, 18.9 mmol) was added to a solution of **5** (2.53 g, 2.36 mmol) in THF (50 mL). The reaction mixture was stirred for 14 h in the absence of light. The precipitate was collected on a fritted funnel and rinsed with THF and CH_2Cl_2. The limited stability of oligomer **6** did not allow its proper characterization by NMR, so it was dried and used directly in the next step without further purification.

*2.3.5. Synthesis of N,N′-bis-(2-ethylhexyl)-3,3′-(5-bromo-thieno [3,2-b]thiophen-2-yl)isoindigo (**7**)*

To a solution of compound **6** (1.6 g, 2.1 mmol) in THF (60 mL), *N*-bromosuccinimide (NBS, 783 mg, 4.4 mmol) was added in several portions in the dark. The reaction mixture was stirred at room temperature for 10 h. Then it was poured into water and extracted with diethyl ether. Removal of the solvent and column purification on silica gel afforded the target compound **7** (0.98 g, 51%). ^{1}H NMR (600 MHz, $CDCl_3$) δ 9.17 (d, $J = 8.4$ Hz, 2H), 7.48 (s, 2H), 7.28 (d, $J = 8.4$ Hz, 2H), 7.26 (s, 2H), 6.95 (s, 2H), 3.71 (m, 4H), 1.88 (m, 2H), 1.44–1.25 (m, 16H), 0.92–0.90 (m, 12H); ^{13}C NMR (150 MHz, $CDCl_3$) δ 168.6, 145.8, 145.3, 140.3, 138.1, 137.7, 132.0, 130.4, 122.3, 121.4, 119.2, 115.9, 114.2, 105.0, 44.4, 37.8, 31.0, 28.9, 25.2, 23.0, 13.6, 10.8; IR (KBr, cm^{-1}): 1690 (C=O), 1611 (C=C); APCI-MS $[M + H]^+$ calculated for $C_{44}H_{45}Br_2N_2O_2S_4^+$ *m/z*: 921.0707, found: 921.0732.

*2.3.6. Synthesis of the oligomer **IDTTT***

In a 25 mL dry flask, compound **7** (276 mg, 0.30 mmol), **8** (431 mg, 1.2 mmol), $Pd(PPh_3)_4$ (28 mg) were dissolved in degassed toluene (20 mL). The mixture was vigorously stirred at 100 °C under nitrogen for 24 h. After cooling to room temperature, the aqueous layer was extracted with dichloromethane. The organic layer was washed with water and brine and then dried over anhydrous $MgSO_4$. After removal of the solvent by vacuum evaporation, the residue was purified by column chromatography on silica gel (214 mg, 62%). ^{1}H NMR (600 MHz, $CDCl_3$) δ 9.08 (d, $J = 8.4$ Hz, 2H), 7.42 (s, 2H), 7.22 (d, $J = 8.4$ Hz, 2H), 7.19 (s, 2H), 7.00 (d, $J = 3.6$ Hz, 2H), 6.83 (s, 2H), 6.66 (d, $J = 3.6$ Hz, 2H), 3.67 (m, 4H), 2.73 (d, $J = 6.6$ Hz, 4H), 1.83 (m, 2H), 1.60–1.25 (m, 34H), 0.97 (m, 6H), 0.92–0.89 (m, 18H); ^{13}C NMR (150 MHz, $CDCl_3$) δ 168.7, 145.6, 145.1, 144.9, 140.7, 140.0, 138.5, 137.9, 135.0, 131.6, 130.2, 126.0, 123.8, 121.2, 118.8, 116.4, 114.9, 104.5, 44.1, 41.4, 37.8, 34.2, 32.4, 30.9, 28.9, 28.8, 25.5, 24.3, 23.1, 23.0, 14.1, 11.0, 10.9, 10.8; IR (KBr, cm^{-1}): 1686 (C=O), 1610(C=C); APCI-MS

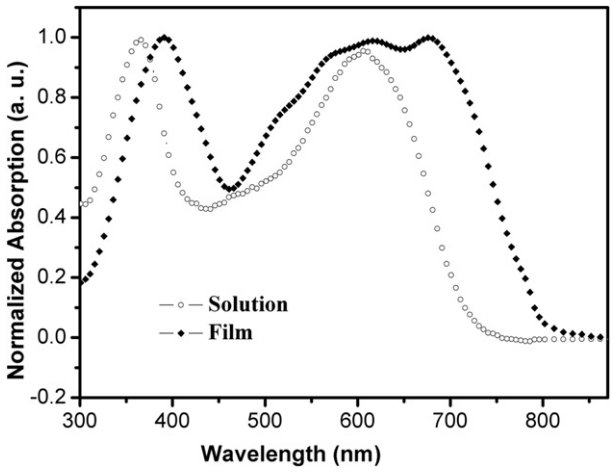

Fig. 2. Absorption spectra of IDTTT in solution and in film.

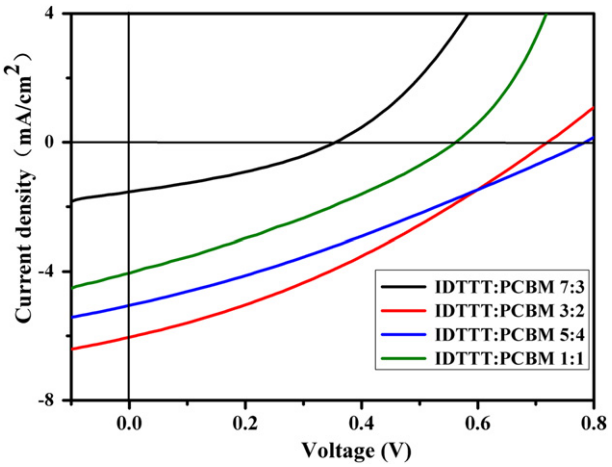

Fig. 4. *J*–*V* curves of photovoltaic devices based on four blends of IDTTT:PCBM (7:3, 3:2, 5:4, and 1:1) (wt/wt) under AM 1.5G illumination.

$[M + H]^+$ calculated for $C_{68}H_{83}N_2O_2S_6^+$ *m/z*: 1151.4773, found: 1151.4791; UV–vis (CH_2Cl_2) λ_{max} (ε [$\times 10^3$ M^{-1} cm^{-1}]) 361 (6.5), 495 (7.5), 605 (12) nm.

3. Results and discussion

3.1. Optical properties

Fig. 2 shows the normalized UV–vis absorption spectra of the oligomer IDTTT in dilute $CHCl_3$ solution (10^{-5} M) and in thin film. In chloroform, IDTTT exhibits strong optical absorption, with two peaks at 363 and 605 nm, respectively, and the extinction coefficient is about 1.2×10^4 L mol^{-1} cm^{-1} (at 605 nm). The short-wavelength absorption peak is ascribed to the delocalized excitonic π–π* transition in the conjugated chains and the long-wavelength absorption peak is attributed to the intramolecular charge transfer (ICT) between the isoindigo and thieno[3,2-*b*] thiophene (TT) units [40]. Remarkably, the absorption of IDTTT in the thin solid film shows a broad absorption from 300 to 800 nm, with the maximum peak at 677 nm, about 72 nm red-shifted compared to that recorded in solution. The spectrum of the film shows large shoulders at 575 and 625 nm, respectively, which generally indicate a strong intermolecular packing occurred in the solid state caused by their planar and rigid backbones [41]. The optical bandgap estimated from the absorption edge of the thin film is 1.54 eV. This value is in accordance with optimum bandgap (1.5 eV) for BHJ cells suggested by theoretical calculations [19].

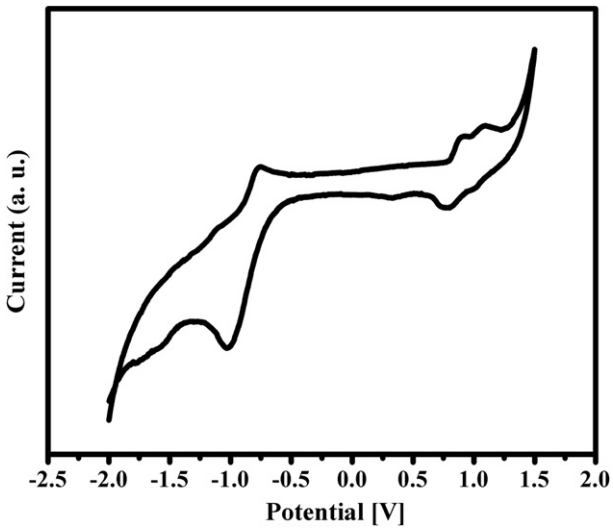

Fig. 3. Cyclic voltammetry of IDTTT measured in a 0.1 M solution of $TBAPF_6$/DCM (scan rate 100 mV/s) *vs* Ag/AgCl electrode.

3.2. Electrochemical characteristics

The oxidation and reduction of IDTTT were measured by cyclic voltammetry (CV). The CV curve was recorded in dichloromethane with tetrabutylammonium hexafluorophosphate ($TBAPF_6$, 0.1 M) as electrolyte at a scan rate of 100 mV/s against an Ag/AgCl reference electrode (Fig. 3). As external standard the redox couple ferrocene/ferrocenium was used. The HOMO and LUMO levels are estimated from the onset of the oxidation and reduction wave assuming the energy level of ferrocene/ferrocenium at −4.8 eV relative to the vacuum level. Thus the HOMO and LUMO levels for IDTTT are −5.39 and −3.92 eV, respectively, and the electrochemical bandgap calculated from the gap between the onset potentials of oxidation and reduction is 1.47 eV, which is close to the optical bandgap (1.54 eV).

An empirical equation describing the relationship between V_{OC} and the energy levels of both the donor and acceptor was derived by Scharber et al. by examining several polymer systems. This derivation is based on a statistical analysis between V_{OC} and ΔE_{DA} (the energy offset between the donor and acceptor, Eq. (1)) [15].

$$V_{oc} = (1/e)(E_{\text{Donor}}\text{HOMO} - E_{\text{PCBM}}\text{LUMO}) - 0.3\ \text{V} \quad (1)$$

Here, *e* is the elementary charge. The value of 0.3 V in Eq. (1) is an empirical factor. Also, this correlation is oversimplified as other important factors may need to be taken into consideration, such as molecular structures and morphology. However, it implies the relation between V_{OC} and the HOMO of the donor. The relatively

Table 1
The photovoltaic performance for the IDTTT/PCBM blending with different ratios.

Active layer (w/w)	J_{SC} (mA/cm^2)	V_{OC} (V)	*FF* (%)	PCE (%)
IDTTT:PCBM (7:3)	1.54	0.36	33.9	0.20
IDTTT:PCBM (3:2)	6.03	0.72	32.5	1.41
IDTTT:PCBM (5:4)	5.04	0.78	29.4	1.27
IDTTT:PCBM (1:1)	4.04	0.56	31.3	0.76

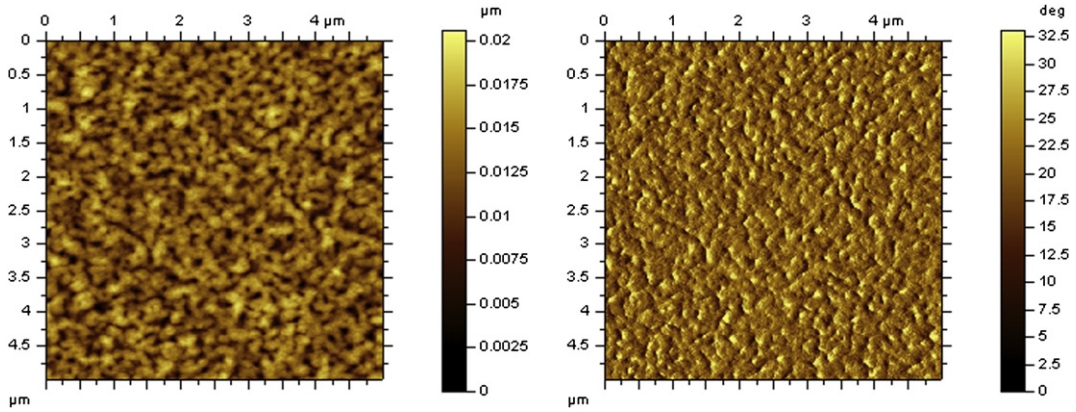

Fig. 5. AFM images (5 μm × 5 μm) of blend film (IDTTT:PCBM = 3:2, w/w) spin-coated on ITO substrate from chlorobenzene solution (left: height image; right: phase image).

low lying HOMO level (−5.39 eV) of IDTTT is expected to endow the donor not only with good chemical stability under ambient conditions, but also a high V_{OC} of the resulted BHJ solar cells based on the molecule. On the basis of these optical and electronic measurements, one can assume that IDTTT with a low bandgap and a low lying HOMO level is a viable candidate for application in OPVs.

3.3. Photovoltaic properties

Bulk heterojunction solar cells were fabricated in the device configuration ITO/ZnO/IDTTT:PCBM/MoO_3/Ag by solution processing method. The *J*–*V* curves of the cells based on IDTTT:PCBM with four different weight ratios of 7:3, 3:2, 5:4 and 1:1 under illumination are shown in Fig. 4. For the four devices, the PCEs are 0.20%, 1.41%, 1.27%, and 0.76%, respectively (Table 1). The device for a 1:1 blend ratio exhibits a moderate PCE. But increasing the donor–acceptor blend ratios from 1:1 to 5:4, 3:2 and 7:3, the J_{SC} firstly increases and then decreases. It was possible that in the case of a low amount of PCBM, such as for 7:3 (wt/wt), it is difficult to form an interpenetrating network morphology for exciton diffusing and dissociating at the interface between donor and acceptor. As the PCBM amount increases, such as for 1:1 (wt/wt), aggregation may be occurring, which can inhibit exciton generation, separation and transport in the device. The device of a blend ratio of 3:2 displays the best performance which gives a J_{SC} of 6.03 mA/cm^2, a V_{OC} of 0.72 V, a fill factor (FF) of 32.5%, and thus a PCE of 1.41% is obtained.

Although IDTTT shows ideal bandgap and HOMO level, moderate performance was obtained unexpectedly. In order to better understand the reason, atomic force microscopy (AFM) was employed to investigate the morphology of blend film (IDTTT:PCBM = 3:2, w/w), where the images were obtained in a surface area of 5 × 5 μm^2 by the tapping mode. Fig. 5 reveals that the root-mean-square roughness (RMS) of the film is about 2.7 nm. The rough surface would not facilitate charge separation [42]. It is also well known that an interpenetrating bicontinuous network between oligomer and PCBM with a domain size of 10–20 nm is important for high performance OPVs [43]. Larger domain sizes of the blend films are not favorable for efficient charge transfer and separation [44]. The morphology exhibits large domains which would increase the possibility for charge recombination (Fig. 5). In addition, height image reveals distinct phase separation which implies poor miscibility between the oligomer and PCBM. Compared to IDTTT, the isoindigo-based oligomer reported by Reynolds exhibits more smooth surface (with RMS of 0.15 nm as-cast) [27]. The result indicates that integrating thieno[3,2-*b*]thiophene into conjugated chain can tune the bandgap and HOMO to an ideal level, however, it also decreases the solubility of the oligomer, thus the miscibility with PCBM is inhibited, and the rough surface and large domains are obtained, which is probably the main reason for poor PCE of the cells, although the energy levels of the molecule match well with that of acceptor PCBM. A modification of the molecule for further improving solubility but retaining its electro-optical properties would be necessary.

4. Conclusion

In conclusion, we applied an easy strategy to control the bandgap and energy levels of a molecule, following which extended π-conjugated unit was incorporated into isoindigo, thus an isoindigo-based oligomer IDTTT has been synthesized and characterized. The compound featured a low bandgap (~1.5 eV) and a low lying HOMO energy level (−5.39 eV), both of which were ideal for photovoltaic application. The absorption spectra of IDTTT covered a large fraction of solar spectrum which suggested it be a good donor candidate for OPVs. The photovoltaic device based on IDTTT as the donor and PCBM as the acceptor exhibited a preliminary PCE of up to 1.41% using a straightforward inverted structure, validating that isoindigo was a promising electron-deficient building block for constructing D–A type of donor materials. The result is inferior to our expectation probably due to serious phase separation because of low miscibility with PCBM. Further improvement in photovoltaic performance can be expected by optimizing the electron rich units of the isoindigo-based D–A structures.

Acknowledgments

This work was supported by National Natural Science Foundation of China (21274134, 51173199, 61107090), the Ministry of Science and Technology of China (2010DFA52310), CAS ("One Hundred Talented Program", and KGCX2-YW-399+9-2), Department of Science and Technology of Shandong Province (2010GGC10345), Shandong Provincial Natural Science Foundation (ZR2011BZ007), Qingdao Municipal Science and Technology Program (11-2-4-22-hz), and New Century Excellent Talents in University (NCET-11-0473).

References

[1] Jo JW, Kim SS, Jo WH. Synthesis of thieno[3,4-d]thiazole-based conjugated polymers and HOMO level tuning for high photovoltaic cell. Org Electron 2012;13:1322–8.
[2] Cheng YJ, Yang SH, Hsu CS. Synthesis of conjugated polymers for organic solar cell applications. Chem Rev 2009;109:5868–923.

[3] Zhen HY, Li K, Huang Z, Tang Z, Wu R, Li G, et al. Inverted indium-tin-oxide-free cone-shaped polymer solar cells for light trapping. Appl Phys Lett 2012; 100:213901–4.
[4] Dennler G, Scharber MC, Brabec CJ. Polymer-fullerene bulk-heterojunction solar cells. Adv Mater 2009;21:1323–38.
[5] He ZC, Zhong CM, Huang X, Wong WY, Wu HB, Chen LW, et al. Simultaneous enhancement of open-circuit voltage, short-circuit current density, and fill factor in polymer solar cells. Adv Mater 2011;23:4636–43.
[6] Zhou HX, Yang LQ, Stuart AC, Price SC, Liu SB, You W. Development of fluorinated benzothiadiazole as a structural unit for a polymer solar cell of 7% efficiency. Angew Chem Int Edit 2011;50:2995–8.
[7] Liang YY, Xu Z, Xia JB, Tsai ST, Wu Y, Li G, et al. For the bright future-bulk heterojunction polymer solar cells with power conversion efficiency of 7.4%. Adv Mater 2010;22:E135–8.
[8] Dou LT, You JB, Yang J, Chen CC, He YJ, Murase S, et al. Tandem polymer solar cells featuring a spectrally matched low-bandgap polymer. Nat Photonics 2012;6:180–5.
[9] Mayukh M, Jung IH, He F, Yu LP. Incremental optimization in donor polymers for bulk heterojunction organic solar cells exhibiting high performance. J Polym Sci Part B-Polym Phys 2012;50:1057–70.
[10] Liu YS, Wan XJ, Wang F, Zhou JY, Long GK, Tian JG, et al. Spin-coated small molecules for high performance solar cells. Adv Energy Mater 2011;1:771–5.
[11] Sharma GD, Mikroyannidis JA, Sharma SS, Roy MS, Thomas KRJ. Efficient bulk heterojunction photovoltaic devices based on diketopyrrolopyrrole containing small molecule as donor and modified PCBM derivatives as electron acceptors. Org Electron 2012;13:652–66.
[12] Wang SS, Bian ZQ, Xia XY, Huang CH. Heterojunction organic solar cells based on donor-pi-acceptor small molecule layers with controlled interface morphology. Org Electron 2010;11:1909–15.
[13] Sun YM, Welch GC, Leong WL, Takacs CJ, Bazan GC, Heeger AJ. Solution-processed small-molecule solar cells with 6.7% efficiency. Nat Mater 2012;11:44–8.
[14] Van der Poll TS, Love JA, Nguyen TQ, Bazan GC. Non-basic high-performance molecules for solution-processed organic solar cells. Adv Mater 2012;24: 3646–9.
[15] He F, Yu LP. How far can polymer solar cells go? In need of a synergistic approach. J Phys Chem Lett 2011;2:3102–13.
[16] Zhou HX, Yang LQ, Liu SB, You W. A tale of current and voltage interplay of band gap and energy levels of conjugated polymers in bulk heterojunction solar cells. Macromolecules 2010;43:10390–6.
[17] Scharber MC, Wuhlbacher D, Koppe M, Denk P, Waldauf C, Heeger AJ, et al. Design rules for donors in bulk-heterojunction solar cells – towards 10% energy-conversion efficiency. Adv Mater 2006;18:789–94.
[18] Soci C, Hwang IW, Moses D, Zhu Z, Waller D, Gaudiana R, et al. Photoconductivity of a low-bandgap conjugated polymer. Adv Funct Mater 2007;17:632–6.
[19] Zhou HX, Yang LQ, Stoneking S, You W. A weak donor-strong acceptor strategy to design ideal polymers for organic solar cells. ACS Appl Mater Interfaces 2010;2:1377–83.
[20] Fitzhugh EW. Artists' pigments: a handbook of their history and characteristics, vol. 4; 1997.
[21] Wienk MM, Turbiez M, Gilot J, Janssen RAJ. Narrow-bandgap diketopyrrolopyrrole polymer solar cells: the effect of processing on the performance. Adv Mater 2008;20:2556–660.
[22] Bijleveld JC, Zoombelt AP, Mathijssen SGJ, Wienk MM, Turbiez M, de Leeuw DM, et al. Poly(diketopyrrolopyrrole-terthiophene) for ambipolar logic and photovoltaics. J Am Chem Soc 2009;131:16616–7.
[23] Zhou EJ, Wei QS, Yamakawa S, Zhang Y, Tajima K, Yang CH, et al. Diketopyrrolopyrrole-based semiconducting polymer for photovoltaic device with photocurrent response wavelengths up to 1.1 μm. Macromolecules 2010;43:821–6.
[24] Ashraf RS, Chen ZY, Leem DS, Bronstein H, Zhang WM, Schroeder B, et al. Silaindacenodithiophene semiconducting polymers for efficient solar cells and high-mobility ambipolar transistors. Chem Mater 2011;23:768–70.
[25] Zhang GB, Du YY, Xie ZY, Zhang Q. Synthesis and photovoltaic properties of new low bandgap isoindigo-based conjugated polymers. Macromolecules 2011;44:1414–20.
[26] Wang EG, Ma ZF, Zhang Z, Vandewal K, Henriksson P, Inganas O, et al. An easily accessible isoindigo-based polymer for high-performance polymer solar cells. J Am Chem Soc 2011;133:14244–7.
[27] Mei JG, Graham KR, Stalder R, Reynolds JR. Synthesis of isoindigo-based oligothiophenes for molecular bulk heterojunction solar cells. Org Lett 2010;12: 660–3.
[28] Afonina I, Skabara PJ, Vilela F, Kanibolotsky AL, Forgie JC, Bansal AK, et al. Synthesis and characterisation of new diindenodithienothiophene (DITT) based materials. J Mater Chem 2010;20:1112–6.
[29] Gao P, Cho D, Yang XY, Enkelmann V, Baumgarten M, Mullen K. Heteroheptacenes with fused thiophene and pyrrole rings. Chem-Eur J 2010;16: 5119–28.
[30] Shinamura S, Miyazaki E, Takimiya K. Crystal structures and semiconductor characteristics of naphtho[1,2-*b*:5,6-*b*′]dithiophene and diselenophene derivatives. J Org Chem 2010;75:1228–34.
[31] Shahid M, Ashraf RS, Klemm E, Sensfuss S. Synthesis and properties of novel low-band-gap thienopyrazine-based poly(heteroarylenevinylene)s. Macromolecules 2006;39:7844–53.
[32] Radke KR, Ogawa K, Rasmussen SC. Highly fluorescent oligothiophenes through the incorporation of central dithieno[3,2-*b*:2′,3′-*d*]pyrrole units. Org Lett 2005;7:5253–6.
[33] Ogawa K, Rasmussen SC. N-functionalized poly(dithieno[3,2-*b*:2′,3′-*d*]pyrrole)s: highly fluorescent materials with reduced band gaps. Macromolecules 2006;39:1771–8.
[34] Huang JS, Chou CY, Liu MY, Tsai KH, Lin WH, Lin CF. Solution-processed vanadium oxide as an anode interlayer for inverted polymer solar cells hybridized with ZnO nanorods. Org Electron 2009;10:1060–5.
[35] Hadipour A, de Boer B, Wildeman J, Kooistra FB, Hummelen JC, Turbiez MGR, et al. Solution-processed organic tandem solar cells. Adv Funct Mater 2006; 16:1897–903.
[36] Dennler G, Prall HJ, Koeppe R, Egginger M, Autengruber R, Sariciftci NS. Enhanced spectral coverage in tandem organic solar cells. Appl Phys Lett 2006;89:073502–4.
[37] Jung SH, Kim HK, Kim SH, Kim YH, Jeoung SC, Kim D. Palladium-catalyzed direct synthesis, photophysical properties, and tunable electroluminescence of novel silicon-based alternating copolymers. Macromolecules 2000;33: 9277–88.
[38] Stalder R, Mei JG, Reynolds JR. Isoindigo-based donor-acceptor conjugated polymers. Macromolecules 2010;43:8348–52.
[39] Zhang GB, Fu YY, Zhang Q, Xie ZY. Benzo[1,2-*b*:4,5-*b*′]dithiophene–dioxopyrrolothiophen copolymers for high performance solar cells. Chem Commun 2010;46:4997–9.
[40] Cho S, Seo JH, Kim SH, Song S, Jin Y, Lee K, et al. Effect of substituted side chain on donor–acceptor conjugated copolymers. Appl Phys Lett 2008;93:263301–3.
[41] Yin B, Yang LY, Liu YS, Chen YS, Qi QJ, Zhang FL, et al. Solution-processed bulk heterojunction organic solar cells based on an oligothiophene derivative. Appl Phys Lett 2010;97:023303–6.
[42] Zhang Y, Zou J, Yip H-L, Chen K-S, Davies J, Sun Y, et al. Synthesis, characterization, charge transport, and photovoltaic properties of dithienobenzoquinoxaline- and dithienobenzopyridopyrazine-based conjugated polymers. Macromolecules 2011;44:4752–8.
[43] Guo X, Zhang M, Tan J, Zhang S, Huo L, Hu W, et al. Influence of D/A ratio on photovoltaic performance of a highly efficient polymer solar cell system. Adv Mater 2012;24:6536–41.
[44] Nie W, MacNeill CM, Li Y, Noftle RE, Carroll DL, Coffin RC. A soluble high molecular weight copolymer of benzo[1,2-*b*:4,5-*b*′]dithiophene and benzoxadiazole for efficient organic photovoltaics. Macromol Rapid Commun 2011; 32:1163–8.